Perfusion MR Imaging: Clinical Utility for the Differential Diagnosis of Various Brain Tumors

Sung Ki Cho, MD[1]
Dong Gyu Na, MD[1]
Jae Wook Ryoo, MD[1]
Hong Gee Roh, MD[1]
Chan Hong Moon, PhD[1]
Hong Sik Byun, MD[1]
Jong Hyun Kim, MD[2]

Objective: To determine the utility of perfusion MR imaging in the differential diagnosis of brain tumors.

Materials and Methods: Fifty-seven patients with pathologically proven brain tumors (21 high-grade gliomas, 8 low-grade gliomas, 8 lymphomas, 6 hemangioblastomas, 7 metastases, and 7 various other tumors) were included in this study. Relative cerebral blood volume (rCBV) and time-to-peak (TTP) ratios were quantitatively analyzed and the rCBV grade of each tumor was also visually assessed on an rCBV map.

Results: The highest rCBV ratios were seen in hemangioblastomas, followed by high-grade gliomas, metastases, low-grade gliomas, and lymphomas. There was no significant difference in TTP ratios between each tumor group ($p>0.05$). At visual assessment, rCBV was high in 17 (81%) of 21 high-grade gliomas and in 4 (50%) of 8 low-grade gliomas. Hemangioblastomas showed the highest rCBV and lymphomas the lowest.

Conclusion: Perfusion MR imaging may be helpful in the differentiation of the various solid tumors found in the brain, and in assessing the grade of the various glial tumors occurring there.

Index terms:
Brain neoplasms, diagnosis
Brain neoplasms, MR
Brain, perfusion
Magnetic resonance (MR), perfusion study

Korean J Radiol 2002;3:171-179
Received November 12, 2001; accepted after revision April 18, 2002.

Departments of [1]Radiology and [2]Neurosurgery, Samsung Medical Center, Sungkyunkwan University School of Medicine

Address reprint requests to:
Hong Sik Byun, MD, Department of Radiology, Samsung Medical Center, Sungkyunkwan University School of Medicine, 50 Ilwon-dong, Kangnam-gu, Seoul 135-230, Korea.
Telephone: (822) 3410-2503
Fax: (822) 3410-2559
e-mail: hsbyun@smc.samsung.co.kr

Despite the fact that conventional magnetic resonance (MR) imaging following the injection of gadolinium (Gd)-based contrast agents has led to improved accuracy in the detection and characterization of various brain tumors, the procedure suffers certain limitations related to the nonspecificity of contrast enhancement. Specifically, this does not provide a clear-cut differential diagnosis between high- and low-grade tumors, between radiation necrosis and proliferating neoplasms, or between postsurgical enhancement and a tumor that infiltrates the margins of the surgical bed. For these reasons, the clinical role of various functional imaging techniques, including nuclear medicine methodologies such as 18F-fluorodeoxyglucose positron emission tomography (FDG-PET), and functional MRI procedures such as perfusion and diffusion-weighted imaging, and MR spectroscopy, has become an important area of investigation (1).

Among various functional imaging techniques, perfusion MR imaging using a relative cerebral blood volume (rCBV) map is particularly sensitive in depicting microvasculature, and tumor neovascularization can thus be detected (2–4). Several recent studies (5–11) have reported that the potential uses of perfusion MR imaging in the evaluation of brain tumors include tumor grading, the provision of guidance for stereotactic biopsy, differentiation between radiation necrosis and recurrent glioma, and the determination of prognosis and response to treatment. In those studies, the rCBV ra-

tios of high-grade gliomas were significantly higher than those of low-grade gliomas. Lee et al. (12) suggested that the rCBV ratio cutoff value which permitted discrimination between high- and low-grade gliomas was 2.60.

Although recent reports (5−7, 9, 12) of perfusion MR studies of brain tumors have focused on the grading of gliomas, the clinical utility of perfusion MR imaging for the differential diagnosis of various brain tumors has not been established. In this study, we investigated the rCBVs of various brain tumors using perfusion MR imaging and evaluated the utility of this modality in the differential diagnosis of brain tumors.

MATERIALS AND METHODS

Patients

Fifty-seven patients with intracranial tumors confirmed by pathologic examination were included in this study. The group comprised 32 men and 25 women aged 13 to 81 (mean, 44.9) years. All underwent MR imaging prior to treatment, which included surgery, chemotherapy, and radiation therapy. The pathologic diagnosis of the 57 brain tumors included 21 cases of high-grade glioma (12 glioblastoma multiformes, 3 anaplastic astrocytomas, 3 anaplastic oligodendrogliomas, and 3 anaplastic oligoastrocytomas), eight low-grade gliomas (3 oligodendrogliomas, 2 pilocytic astrocytomas, 1 astrocytoma, 1 mixed oligoastrocytoma and 1 pleomorphic xanthoastrocytoma), eight lymphomas, six hemangioblastomas, seven metastases, and seven various other tumors (2 germinomas, 2 medulloblastomas, 1 ganglioglioma, 1 choroid plexus papilloma, and 1 pineal parenchymal tumor). The seven metastatic tumors arose from squamous cell carcinoma of the lung in two patients, and small cell carcinoma of the lung, large cell carcinoma of the lung, and adenocarcinoma of the thyroid, cervix, and rectum in one patient each. For pathologic confirmation, 49 patients underwent total or subtotal tumor resection and all with lymphoma underwent biopsy for the verification of diagnosis. Since gliomas are typically heterogeneous and histologic samples obtained during biopsy may be subject to sampling error (13, 14), we sought to avoid this pitfall by including only gliomas which had undergone subtotal or gross total resection.

Conventional and Perfusion MR Imaging

All patients underwent preoperative conventional and perfusion MR imaging using a 1.5-T imager (Signa, GE Medical Systems, Milwaukee, Wis., U.S.A.). For the latter, we used a gradient-echo single-shot echo-planar imaging (EPI) sequence with the following parameters: TR/ TE, 2000/ 60 msec; flip angle, 90°; field of view, 28×28 cm; 128×128 matrix; section thickness/ gap, 5 mm/ 2 mm. A series of images (10 slices, 50 images/slice) was obtained at 2-second intervals before, during, and after administration of the contrast agent. After 10 seconds, during which time the first five images were acquired and an imaging baseline thus established, a bolus of 15 ml gadopentetate dimeglumine (Magnevist, Schering, Berlin, Germany) was power injected at a rate of 5 ml/second through an 18- or 20-gauge intravenous catheter. In each case, multisection data acquisition was used to record a tumor in its entirety, and a total of 500 images was obtained.

For the postprocessing of perfusion MR data, changes in the relaxation rate ($\Delta R2$) can be calculated from signal intensity using the following equation: $\Delta R2 = -\ln (S/S_0)/TE$, where ln is the natural logarithm, S is signal intensity, and S_0 is baseline signal intensity (15). Tracer recirculation was reduced by fitting a gamma-variate function to the measured $\Delta R2$ curve (15, 16). rCBV maps were generated as gray scale images by numerical integration of the area under a fitted curve on a pixel-by-pixel basis. Time-to-peak (TTP) maps were also obtained as gray scale images from the measured $\Delta R2$ curve on a pixel-by-pixel basis (17, 18).

Table 1. Relative Cerebral Blood Volume Ratios of 57 Brain Tumors

Tumor	No. of Patients	Range	Mean ±SD
High-grade glioma	21	3.02−16.66	9.33±3.96
Low-grade glioma	8	1.30− 5.07	3.64±1.50
Hemangioblastoma	6	18.34−40.75	26.60±8.98
Lymphoma	8	1.38− 2.07	1.80±0.23
Metastasis	7	3.16−13.27	8.34±3.02
Germinoma	2	4.79 and 4.85	4.82
Ganglioglioma	1	5.50	–
Choroid plexus papilloma	1	11.39	–
Pineal parenchymal tumor	1	2.97	–
Medulloblastoma	2	16.08 and 12.45	14.27

Qualitative and Quantitative Analysis

For quantitative analysis, normal white matter within the contralateral hemisphere was used as the internal reference standard (19). To determine maximum rCBV ratios, a region of interest (ROI), including at least 20 pixels, was carefully established in the area of a tumor which according to an rCBV map showed maximal intensity, and also in contralateral normal white matter. A circular ROI was drawn, and measured three times, and its average value was then recorded. The same ROI was also applied to TTP maps. rCBV or TTP ratios were calculated by dividing the mean CBV or TTP of a tumor by that of contralateral normal white matter.

Visual inspection of rCBV map images showed that the signal intensity of all tumors was higher than or similar to that of normal white matter. Thus, after visual grading, we assigned a tumor to the high rCBV group if rCBV maps depicted any intratumoral area with a signal intensity higher than that of gray matter. Similarly, if visual grading showed that the signal intensity of all intratumoral areas was similar to or lower that of gray matter, the tumor was assigned to the low rCBV group. In addition, we assessed the relationship between the visual grades depicted by rCBV maps and the intratumoral enhancement seen at contrast-enhanced T1-weighted imaging.

Statistics

Student's t test was used to determine statistical differences in rCBV or TTP ratios regarding the histopathologic grades of gliomas and to analyze quantitative differences in rCBV ratios between the two groups visually categorized as high or low CBV on rCBV maps. The one-way ANOVA test was used to decide whether rCBV or TTP ratios varied between tumor groups. A p value of less than 0.05 was considered statistically significant.

Table 2. Relative Time-to-peak (TTP) Ratios of 57 Brain Tumors

Tumor	No. of Patients	Range	Mean ±SD
High-grade glioma	21	0.61−1.38	0.98 ±0.15
Low-grade glioma	8	0.71−1.64	1.02 ±0.29
Hemangioblastoma	6	1.03−1.21	1.11 ±0.07
Lymphoma	8	0.98−1.22	1.07 ±0.07
Metastasis	7	1.03−1.34	1.17 ±0.12
Germinoma	2	0.88 and 1.28	1.08
Ganglioglioma	1	1.18	–
Choroid plexus papilloma	1	1.21	–
Pineal parenchymal tumor	1	1.12	–
Medulloblastoma	2	1.09 and 1.12	1.11

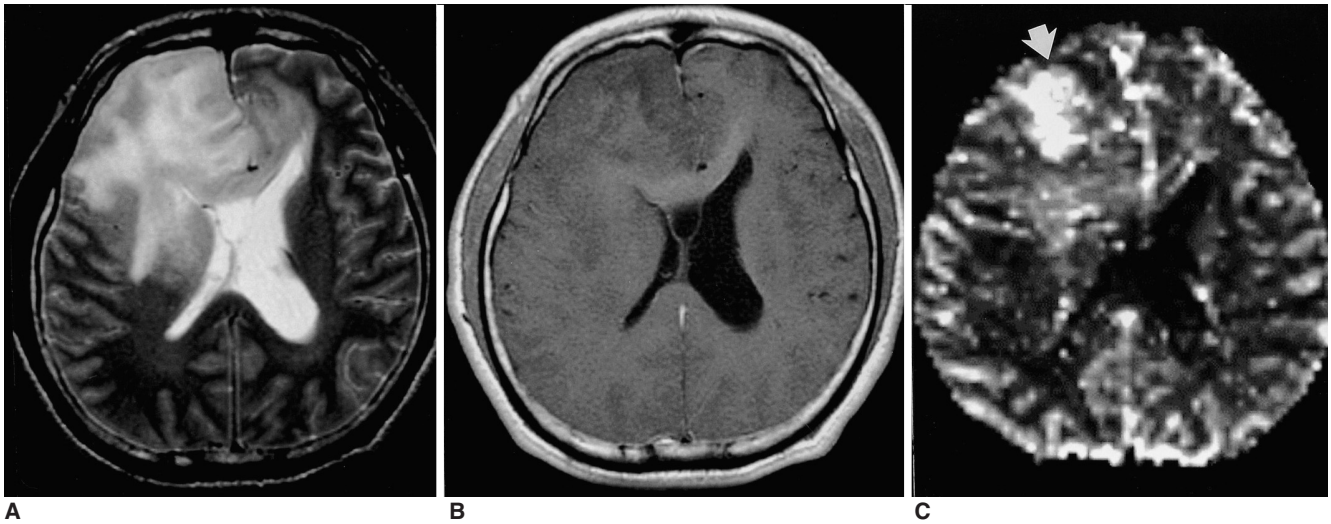

Fig. 1. Malignant mixed oligoastrocytoma in a 30-year-old man. Conventional T2-weighted MR image (**A**) shows a large infiltrative mass with high signal intensity in both frontal lobes and the genu of the corpus callosum. Enhanced T1-weighted MR image (**B**) reveals no contrast enhancement. rCBV map (**C**) depicts foci of increased rCBV within the tumor (arrow). The measured rCBV ratio was 16.27.

RESULTS

rCBV and TTP ratios are summarized in Tables 1 and 2. For high- and low-grade gliomas, these varied from 3.02 to 16.66 (mean ±SD, 9.33 ±3.96) and from 1.30 to 5.07 (mean ±SD, 3.64 ±1.50), respectively (Figs. 1, 2). The difference was statistically significant (p=0.001, Student's t test). In general, the rCBV ratios of high-grade gliomas of a specific histologic type were not significantly different from those of other high-grade gliomas, and this was also the case with low-grade gliomas. Hemangioblastomas showed the highest rCBV ratios (mean, 26.60 ±8.98), which was statistically higher than those of all other tumors (p <0.001). The rCBV ratios of metastases varied from 3.16 to 13.27 (mean, 8.34 ±3.02), a finding similar to that for high-grade gliomas. Lymphomas had low rCBV ratios (Fig. 3), ranging from 1.38 to 2.07, values which were significantly lower than those of high-grade gliomas (p =0.001) or metastases (p =0.032) (Fig. 4).

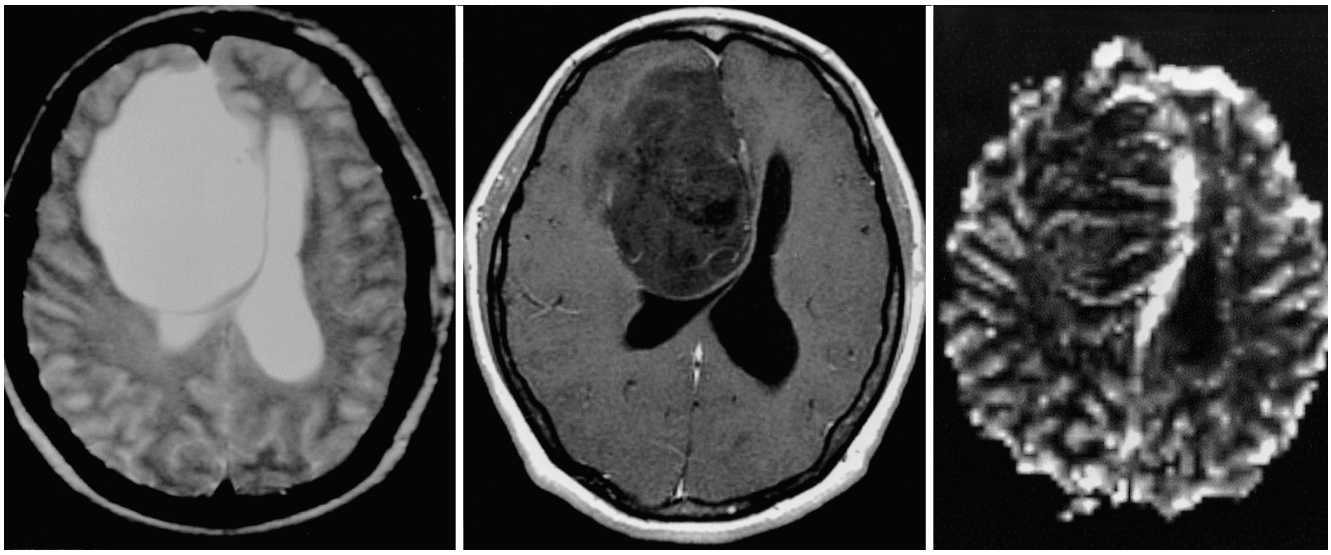

Fig. 2. Low-grade astrocytoma in a 39-year-old woman. Conventional T2-weighted MR image (**A**) reveals the presence of a large infiltrative mass with very high signal intensity in the right frontal lobe. Enhanced T1-weighted MR image (**B**) shows no contrast enhancement. rCBV map (**C**) demonstrates homogeneous low rCBV, the ratio of which was 1.82.

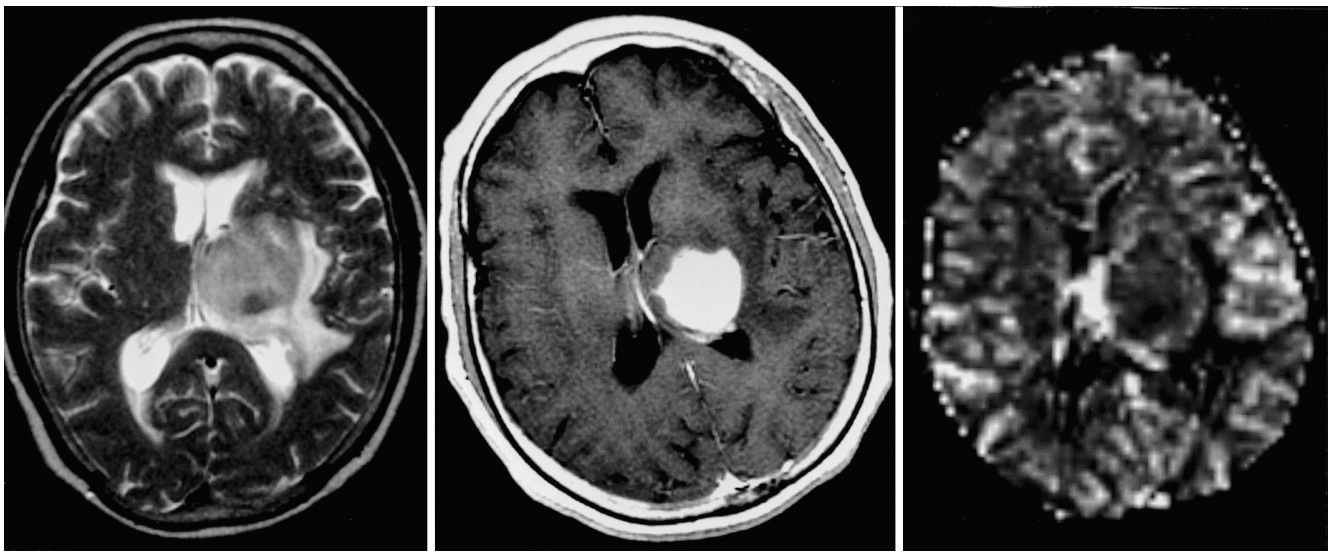

Fig. 3. Diffuse large B-cell lymphoma in a 68-year-old woman. Conventional T2-weighted MR image (**A**) depicts a round mass with intermediate signal intensity in the left thalamus. Enhanced T1-weighted MR image (**B**) demonstrates homogeneous intense enhancement, while rCBV map (**C**) shows homogeneous low rCBV (ratio, 1.72).

The TTP ratios of all tumor groups were similar to those of white matter, and there were no statistically significant differences in TTP ratios between tumor groups ($p > 0.05$).

The relationship between visual grade according to rCBV maps and the intratumoral enhancement seen at contrast-enhanced T1-weighted imaging is summarized in Table 3. At visual assessment of tumors on rCBV maps, a high rCBV was found in 17 (81%) of 21 high-grade gliomas. In five of these 17 patients, however, contrast-enhanced T1-weighted images demonstrated no obvious enhancement within the tumor. Visual examination of rCBV maps showed that four (19%) of 21 high-grade gliomas belonged to the low rCBV group, and in two of these, contrast enhanced T1-weighted images depicted intratumoral enhancement. After visual inspection, four of the eight low-grade gliomas, namely two oligodendrogliomas, one astrocytoma, and one oligoastrocytoma, were assigned to the low rCBV group, and at contrast-enhanced T1-weighte imaging, enhancement of theses tumors was either absent or equivocal. High rCBV was visually determined in two pilocytic astrocytomas, one oligodendroglioma, and one pleomorphic xanthoastrocytoma.

Table 3. The Relationship Between Visual Grades Depicted by Relative Cerebral Blood Volume Maps and Intratumoral Enhancement Seen at Enhanced T1-Weighted Imaging of 57 Brain Tumors

Tumor (Number of Patients)	Number of patients			
	High rCBV on rCBV map		Low rCBV on rCBV map	
	Positive Enhancement at CE MR	Negative Enhancement at CE MR	Positive Enhancement at CE MR	Negative Enhancement at CE MR
High-grade glioma (21)	12	5	2	2
Low-grade glioma (8)	3*	1†	0	4
Lymphoma (8)	0	0	8	0
Hemangioblastoma (6)	6	0	0	0
Metastasis (7)	6	0	1	0
Germinoma (2)	2	0	0	0
Ganglioglioma (1)	1	0	0	0
Choroid plexus papilloma (1)	1	0	0	0
Pineal parenchymal tumor (1)	0	0	1	0
Medulloblastoma (2)	2	0	0	0

Note.—*two pilocytic astrocytomas and one pleomorphic xanthoastrocytoma, †one oligodendroglioma

A **B** **C**

Fig. 4. Metastatic squamous cell carcinoma of the lung in a 56-year-old man. Conventional T2-weighted MR image (**A**) demonstrates a lobulated mass with intermediate signal intensity in the right cerebellum. Enhanced T1-weighted MR image (**B**) shows relatively strong enhancement. rCBV map (**C**) depicts the tumor's relatively high rCBV, the ratio of which was 7.88.

rCBV mapping demonstrated high rCBV in all hemangioblastomas, which at contrast-enhanced T1-weighted imaging showed strong contrast enhancement (Fig. 5). In all lymphomas, on the other hand, low rCBV and strong homogeneous enhancement were apparent. High rCBVs were found in six of seven metastases, each of the two germinomas, each of the two medulloblastomas, the ganglioglioma, and the choroid plexus papilloma. The pineal parenchymal tumor showed low rCBV and contrast enhancement.

The rCBV ratios of tumors assigned at visual examination to the low and the high group ranged from 1.30 to 4.06 (mean, 2.48), and from 4.62 to 40.75 (mean, 12.07), respectively. This difference was statistically significant (p = 0.000).

DISCUSSION

The presence of contrast enhancement at conventional MR imaging represents a pathologic alteration in the blood-brain barrier, with or without concomitant vascular hyperplasia, whereas the degree of MR perfusion abnormality reflects the degree of microvascularity, with or without destruction of the blood-brain barrier (5, 6, 20, 21).

In the grading of gliomas, previous studies (5−7, 9) reported statistically significant differences in rCBV values between low- and high-grade tumors, and demonstrated that high-grade gliomas with high rCBV might not enhance at contrast-enhanced MR imaging. Similar results were obtained in our study. There was a statistically significant difference in rCBV ratios between low- and high-grade gliomas (p =0.001), and five high-grade gliomas with high rCBV showed no obvious contrast enhancement. In our study, four high-grade gliomas had low rCBV, a finding which reflects a low level of neovascularity or contrast leakage through the altered blood-brain barrier. Sugahara et al. (22) reported two cases of anaplastic glioma without increased vascularity, suggesting that a lack of neovascularity within a tumor did not necessarily indicate benignancy. Our results also showed that in two of the four high-grade gliomas with visually determined low rCBV, enhancement was evident at contrast-enhanced T1-weighted MR imaging, a finding which may reflect a falsely low rCBV related to contrast leakage through the altered blood-brain barrier. When this is disrupted, perfusion MR may underestimate the real microvascular blood volume. In a region of severe blood-brain barrier breakdown, unwanted T1 effects caused by extravasated gadolinium counteract the T2 signal-lowering effects of gadolinium, resulting in falsely low rCBV values (23).

Despite their relatively low rCBV ratios, a signal intensity equal to or lower than that of gray matter was apparent at visual analysis of rCBV maps in only four of eight low-grade gliomas; in the other four, rCBV was high. These results may be explained by the relatively high neovascularity of the tumors, revealed at histologic examination. Likewise, previous studies (9, 23) described pilocytic astrocytomas containing foci of high rCBV, and oligodendrogliomas, regardless of their histologic grade, with high blood volume foci. Despite the fact that an oligodendroglioma, independently of its histologic grade, is relative-

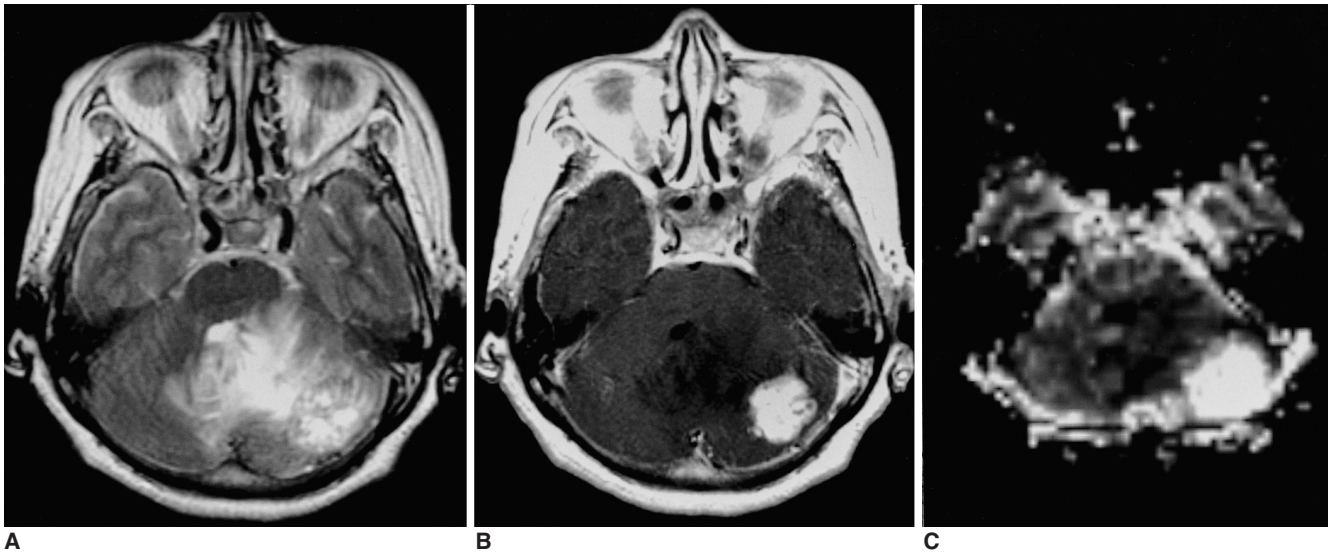

A **B** **C**

Fig. 5. Solid hemangioblastoma in a 62-year-old woman. Conventional T2-weighted MR image (**A**) shows that in the left cerebellum, a lobulated mass with inhomogeneously high signal intensity is present. Enhanced T1-weighted MR image (**B**) shows strong enhancement. rCBV map (**C**) demonstrates very high rCBV (ratio, 40.75).

ly hypervascular, our study demonstrated a statistically significant difference in rCBV ratio between low-grade and anaplastic oligodendroglioma (p =0.009, Student's t test). To clarify this discrepancy, further study of a larger series is, however, necessary.

In our study, a frequently occurring hypervascular tumor such as hemangioblastoma was shown to have an exceedingly high rCBV ratio; this ratio was lowest in lymphomas, in which it was significantly lower than in high-grade gliomas or metastases. Sugahara et al. (24) reported that cerebral lymphomas tended to have lower vascularity than malignant gliomas.

Our study findings suggest that rCBV maps based on perfusion MR imaging data can provide additional information for use in the differential diagnosis of brain tumors. First, they may be useful in differentiating solid cerebellar tumors, including metastatic tumor, lymphoma, and solid hemangioblastoma, in adults; these occasionally show similar conventional MR features of homogeneous enhancement at contrast-enhanced T1-weighted imaging, and intermediate or mild hyperintensity at T2-weighted imaging, though in our cases, quantitative analysis showed indicated that the signal intensity of lymphoma was similar to or lower than that of gray matter, while hemangioblastomas and metastases showed high intensity on rCBV maps of perfusion MR imaging.

Second, an rCBV map is also useful in differentiating cystic astrocytoma from cystic hemangioblastoma. At conventional MR imaging, both cerebellar hemangioblastomas and astrocytomas often appear as small, enhancing nodules

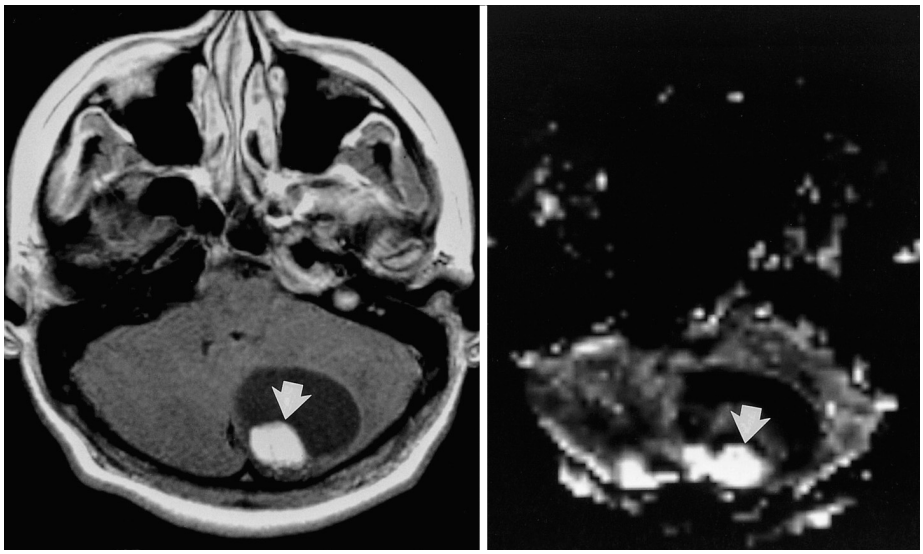

Fig. 6. Cystic hemangioblastoma in a 16-year-old boy. Enhanced T1-weighted MR image (**A**) depicts a cystic mass with a strongly enhancing mural nodule (arrow) in the cerebellum. rCBV map (**B**) reveals very high rCBV (arrow), the measured ratio of which was 34.77.

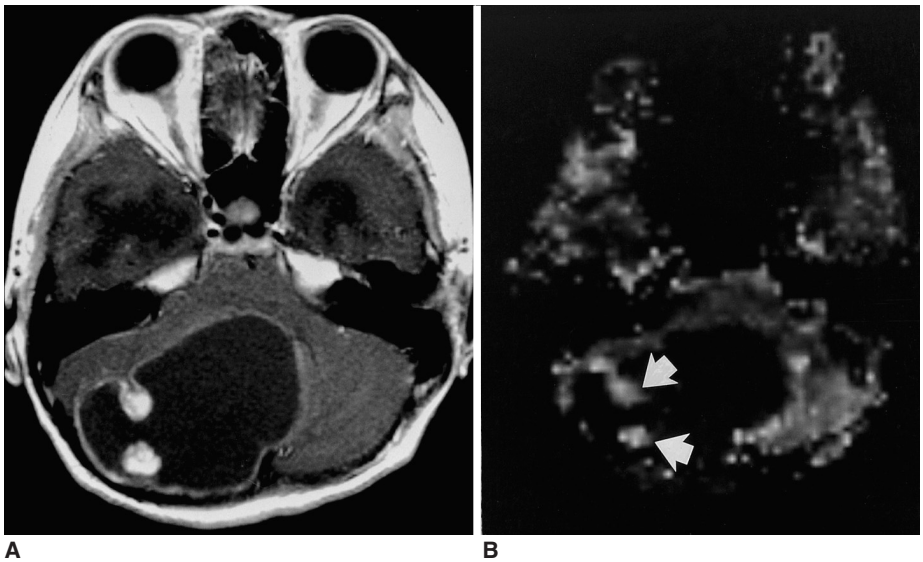

Fig. 7. Pilocytic astrocytoma in a 13-year-old girl. Enhanced T1-weighted MR image (**A**) shows that the cerebellum contains a cystic mass with strongly enhancing mural nodules, similar to the hemangioblastoma shown in Fig. 6. rCBV map (**B**) indicates that the rCBV ratio of these nodules in high (4.65) (arrows), but lower than that of the hemangioblastoma.

within a well circumscribed, thin-walled cyst, as in our cases. Despite some differential features such as an intratumoral signal void, differentiation by conventional MR imaging alone is difficult, especially where tumors are smaller than 1cm (25, 26). Perfusion MR imaging, however, permits differentiation without the need for additional invasive conventional angiography. Quantitative analysis indicated that the rCBV ratio of hemangioblastomas was significantly higher than that of cerebellar astrocytomas, and it was also found that compared with that of gray matter, the signal intensity of hemangioblastomas was higher, while that of cystic astrocytomas was slightly higher (Figs. 6, 7).

Compared to other studies (5–7), the rCBV ratios of tumors in our series were higher in the titer, a fact which may be due to the different way in which ROIs were selected: the ROIs we chose were, for each tumor, in the area which showed maximal perfusion.

Our study findings revealed no differences in TTP between various tumor groups. We noticed that TTP was a useful parameter in stroke cases (27), so sought to identify on TTP maps any differences between various tumor groups, especially between lymphomas and other hypervascular tumors. TTP maps, in contrast to rCBV maps, played only a small part in both the grading and differentiation of the various brain tumors we encountered.

A limitation of this study is the inclusion of only small numbers of cases of low-grade glioma, especially low-grade astrocytoma and oligodendroglioma. To determine the practical utility of perfusion MR imaging in differentiating between low- and high-grade astrocytomas or oligodendrogliomas, further study involving a larger series of these tumors is needed. For the grading of gliomas, determination of a cut-off value for rCBV may be helpful.

In summary, the rCBV ratios of high-grade gliomas were significantly higher than those of low-grade gliomas. For hemangioblastomas, these ratios were exceedingly high; for high-grade gliomas and metastases they were relatively high; and for low-grade gliomas and lymphomas they were relatively low. Visual grading based on rCBV mapping provided added information about tumor characteristics. Perfusion MR imaging may be helpful in the differentiation of the various solid tumors found in the brain, as well as in assessing the grade of the various glial tumors occurring there.

References

1. Brunetti A, Alfano B, Soricelli A, et al. Functional characterization of brain tumors: an overview of the potential clinical value. *Nucl Med Biol* 1996;23:699-715
2. Villringer A, Rosen BR, Belliveau JW, et al. Dynamic imaging with lanthanide chelates in normal brain: contrast due to magnetic susceptibility effects. *Magn Reson Med* 1988;6:164-174
3. Rosen BR, Belliveau JW, Aronen HJ, et al. Susceptibility contrast imaging of cerebral blood volume: human experience. *Magn Reson Med* 1991;22:293-299
4. Belliveau JW, Rosen BR, Kantor HL, et al. Functional cerebral imaging by susceptibility - contrast NMR. *Magn Reson Med* 1990;14:538-546
5. Knopp EA, Cha S, Johnson G, et al. Glial neoplasms: dynamic contrast-enhanced T2*-weighted MR imaging. *Radiology* 1999; 211:791-798
6. Aronen HJ, Gazit IE, Louis DN, et al. Cerebral blood volume maps of gliomas: comparison with tumor grade and histologic findings. *Radiology* 1994;191:41-51
7. Aronen HJ, Glass J, Pardo FS, et al. Echo-planar MR cerebral blood volume mapping of gliomas: clinical utility. *Acta Radiol* 1995;36:520-528
8. Maeda M, Itoh S, Kimura H, et al. Vascularity of meningiomas and neuromas: assessment with dynamic susceptibility-contrast MR imaging. *AJR* 1994;163:181-186
9. Bagley LJ, Grossman RI, Judy KD, et al. Gliomas: correlation of magnetic susceptibility artifact with histologic grade. *Radiology* 1997;202:511-516
10. Siegal T, Rubinstein R, Tzuk-Shina T, Gomori JM. Utility of relative cerebral blood volume mapping derived from perfusion magnetic resonance imaging in the routine follow-up of brain tumors. *J Neurosurg* 1997;86:22-27
11. Wong JC, Provenzale JM, Petrella JR. Perfusion MR imaging of brain neoplasms. *AJR* 2000;174:1147-1157
12. Lee SJ, Kim JH, Kim YM, et al. Perfusion MR imaging in gliomas: comparison with histologic tumor grade. *Korean J Radiol* 2001;2:1-7
13. Russell D, Rubinstein L. T*umours of central neuroepithelial origin*. In: Rubinstein LJ, ed. *Pathology of tumours of the nervous system*. Baltimore: Williams & Wilkins, 1989:83-350
14. Glantz MJ, Burger PC, Herndon JE II, et al. Influence of the type of surgery on the histologic diagnosis in patients with anaplastic gliomas. *Neurology* 1991;41:1741-1744
15. Rosen BR, Belliveau JW, Vevea JM, et al. Perfusion imaging with NMR contrast agents. *Magn Reson Med* 1990;14:249-265
16. Weisskoff R, Belliveau J, Kwong K, Rosen B. *Functional MR imaging of capillary hemodynamics*. In: Potchen E, ed. *Magnetic resonance angiography: concepts and applications*. St Louis: Mosby, 1993:473-484
17. Berchtenbreiter C, Bruening R, Wu RH, et al. Comparison of the diagnostic information in relative cerebral blood volume, maximum concentration, and subtraction signal intensity maps based on magnetic resonance imaging of gliomas. *Invest Radiol* 1999;34:75-81
18. Bitzer M, Klose U, Nagele T, et al. Echo-planar perfusion imaging with high spatial and temporal resolution: methodology and clinical aspects. *Eur Radiol* 1999;9:221-229
19. Di Chiro G, Brooks R, Bairamian D, et al. *Diagnostic and prognostic value of positron emission tomography using [18F] fluorodeoxyglucose in brain tumors*. In: Reivich M, Alavi A, eds. *Positron emission tomography*. New York: Liss, 1985:291-309
20. Brasch RC, Weinmann HJ, Wesbey GE. Contrast-enhanced NMR imaging: animal studies using gadolinium-DTPA complex. *AJR* 1984;142:625-630
21. Grossman I, Wolf G, Biery D, et al. Gadolinium-enhanced nuclear magnetic resonance images of experimental brain abscess. *J Comput Assist Tomogr* 1984;8:204-207

22. Sugahara T, Korogi Y, Kochi M, et al. Correlation of MR imaging-determined cerebral blood volume maps with histologic and angiographic determination of vascularity of gliomas. *AJR* 1998;171:1479-1486
23. Lev MH, Rosen BR. Clinical applications of intracranial perfusion MR imaging. *Neuroimaging Clin North Am* 1999;9:309-331
24. Sugahara T, Korogi Y, Shigematsu Y, et al. Perfusion-sensitive MRI of cerebral lymphomas: a preliminary report. *J Comput Assist Tomogr* 1999;23:232-237
25. Lee SR, Sanches J, Mark AS, Dillon WP, Norman D, Newton TH. Posterior fossa hemangioblastomas: MR imaging. *Radiology* 1989;171:463-468
26. Ho VB, Smirniotopoulos JG, Murphy FM, Rushing EJ. Radiologic-pathologic correlation: hemangioblastoma. *AJNR* 1992;13:1343-1352
27. Martel AL, Allder SJ, Delay GS, Morgan PS, Moody AA. Perfusion MRI of infarcted and noninfarcted brain tissue in stroke: a comparison of conventional hemodynamic imaging and factor analysis of dynamic studies. *Invest Radiol* 2001; 36:378-385